MATERIALS FORUM VOLUME 29 - Published 2005
Edited by J.F. Nie and M. Barnett

OBSERVATION OF DEFORMATION MODES IN Mg-3Al-1Zn

Z. Keshavarz, M.R. Barnett
School of Engineering and Technology, Deakin University, Geelong, VIC 3217, Australia

ABSTRACT

Since magnesium alloys are the lightest metallic materials, they are very attractive for automotive and aerospace industries. The main problem of these alloys is limited ductility due to a shortage of independent slip systems. In order to improve the formability in these alloys, an understanding of the deformation modes is required. In the present work, different slip systems were investigated in rolled Mg-3Al-1Zn by means of in situ tensile tests in the SEM. These permitted electron backscatter diffraction (EBSD) and electron backscatter diffraction imaging (QBSD) to be carried out during the test. The results show that non-basal slip systems are active at room temperature.

1. INTRODUCTION

In magnesium, there are four slip planes considered, (0001) basal, $\{1\bar{1}00\}$ prismatic, $\{1\bar{1}01\}$ first order pyramidal and $\{11\bar{2}2\}$ second order pyramidal planes. For the second order pyramidal slip, the Burgers vector is c+a. Roberts [1] and Raynor [2] have shown that up to 225°C slip occurs readily on the basal planes (0001) of the hexagonal crystal structures, whenever these are favourably oriented in relation to the direction of stress. Above about 225°C additional (pyramidal) slip planes $\{10\bar{1}1\}$ become operative. [3,4] Obara et al. [5] observed the small amount of $\{11\bar{2}2\}\langle\bar{1}\bar{1}23\rangle$ slip systems in magnesium single crystal when deformed under c-axis compression. It was shown by Ward Flynn [6] and Reed-Hill [7] that the critical resolved shear stress for basal and non-basal slip modes decreases, as the temperature increases. The rate of decrease is greater for the non-basal systems. However, small amounts of non-basal slip have been seen after room temperature deformation of pure magnesium [8].

More recently, Agnew et al. [9], Barnett [10] and Staroselsky [11] have found that the inclusion of prismatic and / or second order pyramidal slip in crystal plasticity models is necessary for the simulation of mechanical response of Mg-3Al-1Zn (AZ31) alloy at room temperature.

In present work, the behaviour of different slip systems of Mg-3Al-1Zn at room temperature is investigated using slip line analysis.

2. EXPERIMENTAL PROCEDURES

Flat tensile specimens with a cross section of 10 mm^2 and a gauge length of 25 mm were machined parallel to rolling direction of commercial sample of AZ31 (3% Al, 1% Zn). Before machining, the specimens were annealed for 30 min at 350°C and cooled in air to obtain a stress-free microstructure.

The surface of the tensile specimens was ground with 1200 grit SiC paper. Polishing was then carried out with diamond paste through sequence of 15, 6, 3 and 1 μm. For EBSD mapping, the specimens were mechanically polished with a Colloidal Silica Slurry and etched with a solution of 10 ml HNO_3, 30 ml acetic acid, 40 ml H_2O and 120 ml ethanol for 10 seconds.

Tensile testing was carried out using Kammrath-Weiss in situ tensile stage in a W-filament LEO 1530 scanning electron microscope (SEM) (Figure 1). The stage is small enough to be tilted 70° in the SEM, which allows EBSD patterns to be recorded. During testing, the load was recorded and measurements of the spacing between two markers were periodically carried out for strain calculations. The deformation was performed at 0.5 *μm/s*.

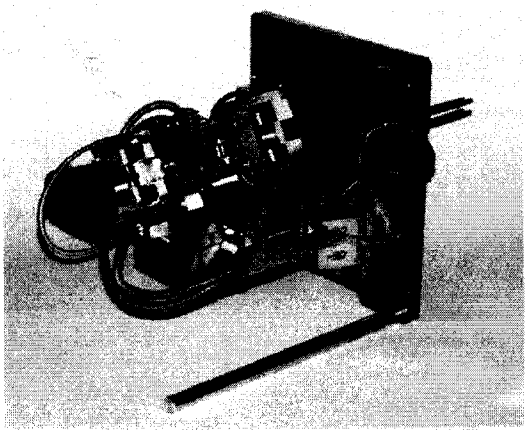

Figure 1: Tensile / compression stage.

3. RESULTS

The texture of the as-received rolled AZ31 was measured by means of EBSD and the basal pole figure obtained is shown in Figure 2. As can be seen, the c-axes are grouped around the normal direction, with some spread towards the rolling direction. This is typical in rolled Mg [12].

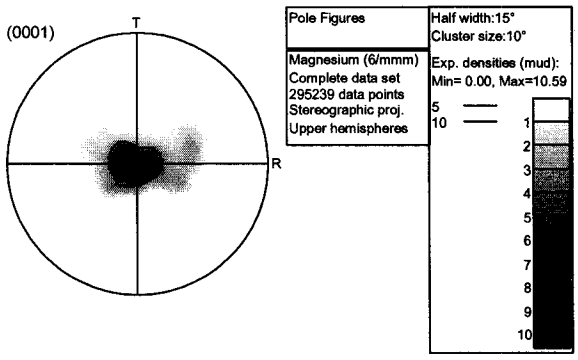

Figure 2: Pole figure taken from the surface of specimen before deformation.

In order to investigate the active slip systems at room temperature, observation by means of SEM and EBSD of the surface of the tensile samples was performed following plastic strains of 0.04, 0.08 and 0.14. A typical stress-strain curve is shown in Figure 3. Different slip traces were observed in different grains and in different deformation stages. To recognize the active slip systems inside of the individual grains, the crystallographic orientation was determined by EBSD and the slip trace orientation was measured from SEM micrographs. After deformation, the surface was not smooth so performing EBSD in every grain was not possible.

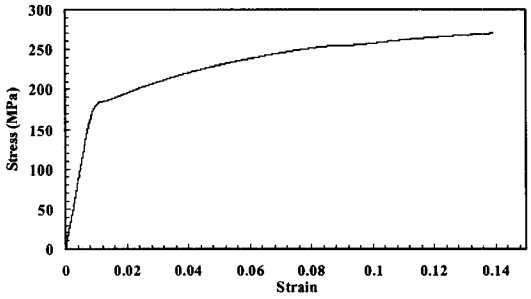

Figure 3: Stress-strain curve of rolled Mg-3Al-1Zn (velocity of 5 μm / s).

Examples of EBSD maps and related pole figures of the slip traces are shown in Figures 4-6. On the pole figure given in Figure 4, the basal pole appears as a point and the intersection of the basal plane with the surface of the sample is shown as a dashed line. In this figure it can be seen that the slip lines are consistent with basal slip. Similar correlation between slip line and basal plane trace was found for 8 of the 19 set of slip lines for which reliable EBSD indexing was obtained. For the 11 other cases, agreement was found between the traces of slip lines and the prismatic plane. Examples of this are presented in Figures 5 and 6. All of the slip lines for which a basal, prismatic or second order pyramidal slip plane trace could be found within 5° are listed in Table 1. The Euler angles are referred to sample axes: 1=RD, 2=TD and 3=ND. The orientations in which basal and prismatic slip systems were observed are presented in Figure 7 by way of inverse pole figures. It can be seen that grains in which basal slip was identified occupy the region where the tensile axis is inclined approximately 45° to the c-axis (<0001> direction). The tensile direction for grains that displayed prismatic slip lies perpendicular to the c-axis.

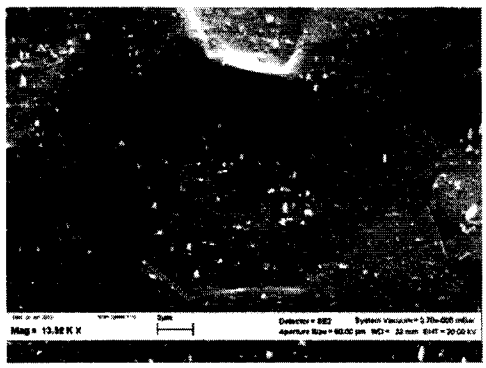

(a)

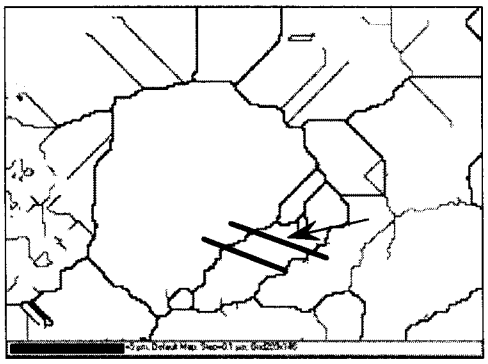

(b)

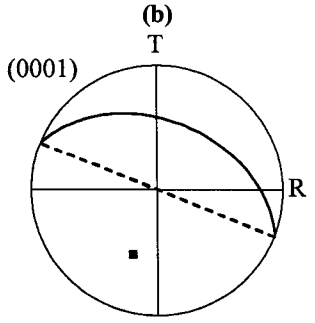

(c)

Figure 4: (a) The slip traces, (b) EBSD map showing the boundaries with a misorientation greater than 15° and (c) pole figure showing expected slip plane trace.

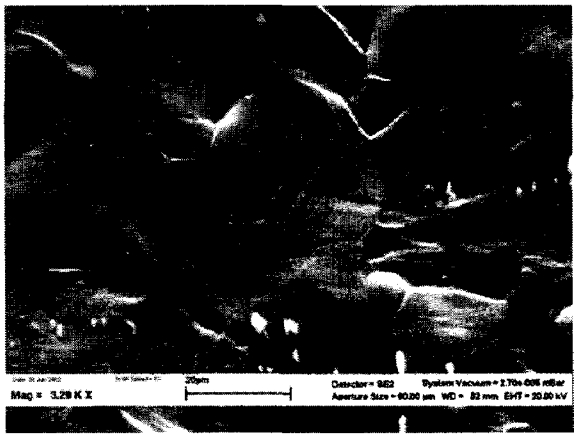

(a)

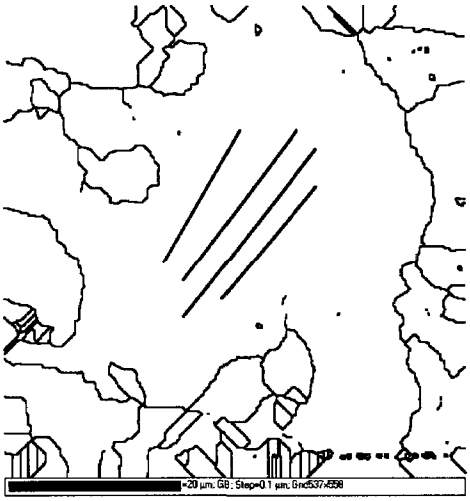

(b)

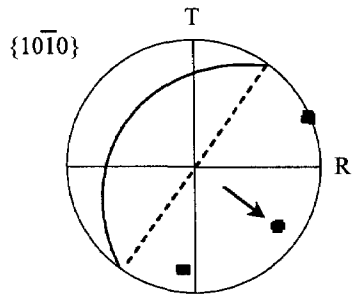

(c)

Figure 5: (a) The slip traces, (b) EBSD map showing the boundaries with a misorientation greater than 15° and (c) pole figure showing expected slip plane trace.

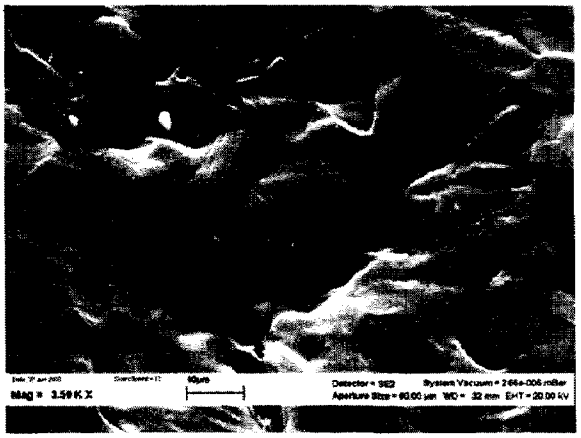

(a)

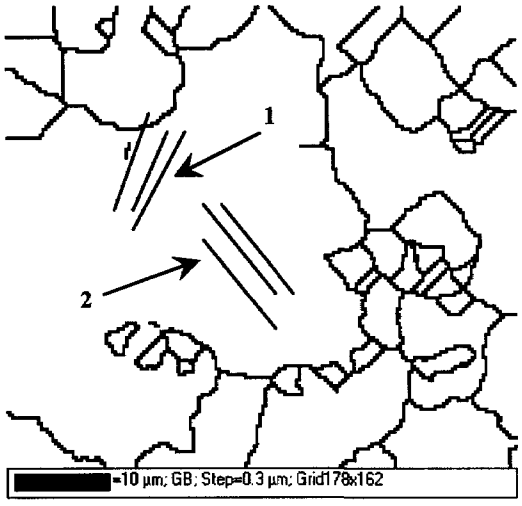

(b)

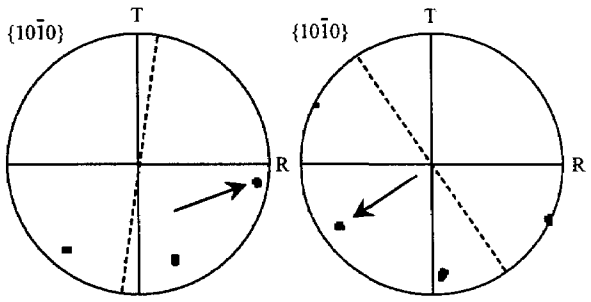

(c) (d)

Figure 6:(a) The slip traces, (b) EBSD map showing the boundaries with a misorientation greater than 15° and pole figure showing expected slip plane traces for (c) set 1 and (d) set 2.

Table 1: Measured Euler angles, observed and computed slip line angle, Schmid factor and strain for each identified slip system.

Strain	Euler Angles $\varphi_1°$	$\phi°$	$\varphi_2°$	Nearest Slip System	Observed Slip Line Angle (to RD)	Deviation from Computed Slip Line Angle (to RD)	Schmid Factor	Next Nearest Slip System	Deviation from Next Nearest Computed Slip Line Angle (to RD)
0.040	66	153	26	basal	63°	3°	0.40	prismatic	7°
0.040	118	32	55	basal	119°	1°	0.36	c+a	5° (Schmid Factor = 0.01)
0.040	114	38	5	basal	115°	1°	0.42	c+a	3° (Schmid Factor = 0.10)
0.040	158	123	55	basal	153°	5°	0.28	c+a	9°
0.040	115	37	3	prismatic	158°	4°	0.28	c+a	8°
0.082	59	38	6	basal	58°	1°	0.39	c+a	6°
0.082	135	52	43	basal	130°	5°	0.44	c+a	10°
0.082	63	41	35	basal	61°	2°	0.47	prismatic	8°
0.082	17	170	45	prismatic	66°	4°	0.42	c+a	20°
0.082	32	166	2	prismatic	115°	5°	0.42	c+a	16°
0.082	30	12	58	prismatic	120°	2°	0.40	c+a	21°
0.142	45	128	12	basal	44°	1°	0.46	c+a	10°
0.142	173	19	54	prismatic	134°	1°	0.50	c+a	18°
0.142	166	18	37	prismatic	57°	3°	0.47	c+a	15°
0.142	34	159	37	prismatic	141°	5°	0.45	c+a	11°
0.142	13	165	22	prismatic	135°	5°	0.49	c+a	15°
0.142	163	11	51	prismatic	67°	3°	0.40	c+a	20°
0.142	14	8	37	prismatic	144°	3°	0.49	c+a	28°
0.142	19	161	26	prismatic	138°	3°	0.48	c+a	14°

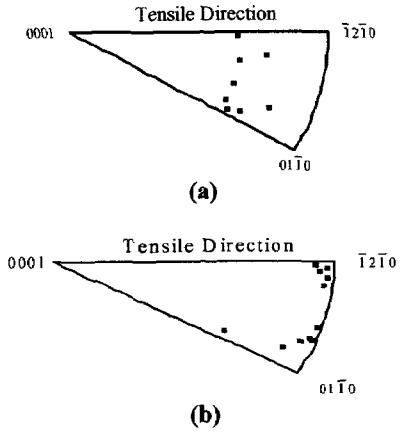

Figure 7: Inverse pole figures of the tensile direction for orientations in which (a) basal and (b) prismatic slip were observed.

4. DISCUSSION

Basal and prismatic slip traces were identified on the surface of the rolled AZ31 specimen during tension along the RD. The identification was based on the proximity of calculated [13] slip plane traces. The next nearest system is identified in Table 1 and it can be seen that, in all bar two cases, the deviation between observation and calculation exceeds the 5° cut off employed in the present work.

The maximum Schmid factors [14] were calculated for each of the slip planes identified and these are also included in Table 1. The Schmid factors in the case of prismatic slip fell between 0.4 and 0.5 (except for one case). The values for basal slip were similarly high.

Detection of slip lines and indexing nearby material were difficult in the present study for three reasons. One, the surface became considerably roughened with increasing strain, which interfered with the indexing of EBSD patterns. Two, the use of the in-situ stage necessitated a high working distance which reduced the ability to resolve slip lines. Three, presence of a large fraction of intermetallic particles masked the slip lines.

These difficulties may account for the fact that basal slip lines were only seen for high Schmid factor orientations despite the well-known ease of basal slip [15]. Workers studying single crystals have observed basal slip even when the basal planes are near to perpendicular to the loading direction, i.e. even when the Schmid factor is very low [15].

The current findings are preliminary. However, they show the importance of prismatic slip in room temperature deformation of Mg-3Al-1Zn. The present findings are in agreement with what has been reported in some recent works (*e.g.* Ref. 9, 10, 16, 17) in which TEM and crystal plasticity have been used to infer the activity of non-basal systems at room temperature. In one of these studies [17], the activity of non-basal slip near grain boundaries was emphasized. In the current study (Figures 5 and 6) prismatic slip was observed well within the grain interior. The significance of this finding is a topic for future study.

5. CONCLUSIONS

Observation of slip systems in tensile samples oriented along the rolling direction, for commercial AZ31 sheet, showed a preference for both non-basal (prismatic) and basal slip during room temperature deformation.

ACKNOWLEDGEMENTS

The technical assistance of Andrew Sullivan and John Vella is gratefully acknowledged. This work was supported by the provision of research scholarship by Deakin University.

REFERENCES

1. C. S. Roberts, Magnesium and Its Alloys (John Wiley & Sons Inc., New York), (1960).
2. G. V. Raynor, The Physical Metallurgy of Magnesium and Its Alloy (Pergamon Press, London), (1959).
3. R. E. Reed-Hill, and W. D. Robertson, Journal of Metals, AIME Trans., 209, 496 (1957).
4. R. E. Reed-Hill, and W. D. Robertson, Transactions of the Metallurgical Society of AIME, 256 (1958).
5. P. Ward Flynn, J. Mote, and J. E. Dorn, Transactions of the Metallurgical Society of AIME, 221, 1148 (1961).
6. R. E. Reed-Hill, and W. D. Robertson, Acta Metallurgica, 5, 728 (1957).
7. S. R. Agnew, M. H. Yoo, and C. N. Tomé, Acta Materialia, 49, 4277 (2001).
8. F. E. Hauser, P. R. Landon, and J. E. Dorn, Trans. Am. Soc. Metals, 50, 856 (1958).
9. S. R. Agnew, Magnesium Technology 2002 - TMS Annual Meeting, Conf. Proc., edited by H. I. Kaplan (TMS, Pennsylvania), pp. 169-174 (2002).
10. M. R. Barnett, Metallurgical and Materials Transactions A, 34A, 1799 (2003).
11. A. Staroselsky, and L. Anand, International Journal of Plasticity, 19, 1843 (2003).
12. Y. N. Wang, and J. C. Huang, Materials Chemistry and Physics, 81 (1), 11 (2003).
13. H. J. Bunge, Texture Analysis in Materials Science (Butterworth & Co., London), pp. 1-41 (1982).
14. C.N. Reid, Deformation Geometry for Materials Scientists (Pergamon Press, Oxford), (1973).
15. F. E. Hauser, P. R. Landon, and J. E. Dorn, Transactions of the ASM, 48, 986 (1956).
16. S. R. Agnew, and O. Duygulu, Magnesium Technology 2004 - TMS Annual Meeting, Conf. Proc., edited by A. A. Luo (TMS, Pennsylvania) pp. 61-65 (2004).
17. J. Koike, T. Kobayashi, T. Mukai, H. Watanabe, M. Suzuki, K. Maruyama, and K. Higashi, Acta Materialia, 51, 2055 (2003).